

# Effect of the Molecular Weight on the Dynamics of the Conformational Transition of Poly(methacrylic acid)

A. F. Olea,<sup>\*,†</sup> H. Rosenbluth,<sup>†</sup> and J. K. Thomas<sup>\*,‡</sup>

*Departamento de Química, Facultad de Ciencias, Universidad de Chile, Casilla 653, Santiago, Chile, and Department of Chemistry & Biochemistry, University of Notre Dame, Notre Dame, Indiana 46556*

*Received March 31, 1999; Revised Manuscript Received September 14, 1999*

**ABSTRACT:** Stop flow pH jump experiments were carried out on poly(methacrylic acid), PMA, solution of various molecular weights. The fluorescence changes of the probe pyrene, which can locate in the hydrophobic PMA coil or in the aqueous phase, were used to monitor pH-induced events in the PMA–water system. At least two well-separated time regions for the pH-induced conformational change of PMA were observed: one with  $\tau = 1\text{--}2$  s and another with  $\tau = 50\text{--}100$  s. A theoretical model to quantitatively explain the observed kinetic changes is given. This is based on a model developed by Schwarz for the helix–coil transition of polypeptides and can be briefly described as follows. Any configuration of the polymer is characterized by a statistical distribution of segments in polar and hydrophobic regions. Then a conformational transition involves the change of a number of segments from one state to the another, and its kinetics corresponds to a relaxation process with the pH jump as the initial perturbation. Several details pertinent to unambiguous interpretation are also described briefly. This includes the rate of neutralization of the acid groups on PMA and the rate of solution of small pyrene crystals in a colloidal system. The above confusing effects were established and thus could be avoided in the actual pH-induced conformational changes of PMA.

## Introduction

The conformational transition of poly(methacrylic acid) (PMA) induced by a change in the degree of ionization has been studied by many workers, all using different techniques.<sup>1–12</sup> The measurement of equilibrium properties, as a function of pH, has established that, at low pH, the macromolecule expands slowly as the charge density increases. At higher pH, after a certain expansion of the coil is achieved, a remarkable expansion of the PMA chain takes place. The transition between these two states occurs at pH 4–6. Despite the large amount of data collected in the past years, the nature of the transition still remains uncertain. Most authors think that this transition is highly cooperative and involves only two mean conformations. However, there is evidence that indicates that a multiplicity of structures exist during the configuration change.<sup>8,11,13</sup> Recently, Heitz et al. have shown that at low pH the conformation of PMA is larger than a compact sphere without water molecules inside it.<sup>12</sup> Also, they found that there is not aggregates in the whole range of pH.

In analogy to the helix–coil transition observed in polypeptides, it has been proposed that the conformational change in synthetic polyelectrolytes is also a consequence of a configuration change of the polymer segments.<sup>1,14,15</sup> In this model, the transition is described as occurring between two forms, A and B, in which the polymer subunits may exist. At low values of  $\alpha$  the form A dominates, and after passing the transition region the B form will occur predominantly. Solubility measurements<sup>3</sup> and fluorescence probing<sup>9–11,16</sup> indicate that the A form is inside a very hydrophobic environment, while the B form is exposed to the aqueous media.<sup>11</sup> Leyte and Mandel<sup>1</sup> assumed that at all  $\alpha$  values a thermodynamic equilibrium exist between the A and B forms. Thus, any

state of the macromolecule can be described as a sequence of A and B segments, and the transition between two different states is represented by a series of unimolecular processes, where a number of subunits are transformed from one form to the another. There are many theoretical studies, based on a statistical thermodynamic model, that describe the equilibrium properties and the kinetics of the transition.<sup>17–19</sup> However, just a few data have been published on the kinetics of the pH-induced conformational transition of synthetic polyelectrolytes.<sup>9,14,15,20–22</sup>

The kinetics of the conformational transition of an alternating maleic acid–styrene copolymer was studied by Ohno et al., and the transition was observed to occur in approximately 500 ms.<sup>14,15</sup> Different fluorescent probes have been used to study the expansion of PMA following a pH jump, where the fluorescence intensity change is assumed to monitor the rate of polymer coil expansion.<sup>9,21,22</sup> Part of the process could not be followed because it was faster than 1 ms, but most of the transition occurs in the range 600–1000 ms. Thus, the conformational transition in synthetic polyelectrolytes is slower than the helix–coil transition of poly( $\alpha$ -amino acid) in solution.<sup>23</sup>

In this paper we present the results of an equilibrium and kinetic study of the conformational transition of PMA as a function of polymer molecular weight, where the molecular weights of these polymers differ by almost 2 orders of magnitude. In the kinetic study, solutions of PMA, at different degrees of dissociation, containing pyrene were mixed with HCl or NaOH in a stopped-flow equipment. The increase of fluorescence intensity of pyrene was monitored until an equilibrium value was reached.

## Experimental Section

**Polymers.** Poly(methacrylic acid) of 100 000 molecular weight (PMAHMW) and poly(methacrylic acid) sodium salt of

<sup>†</sup> Universidad de Chile.

<sup>‡</sup> University of Notre Dame.

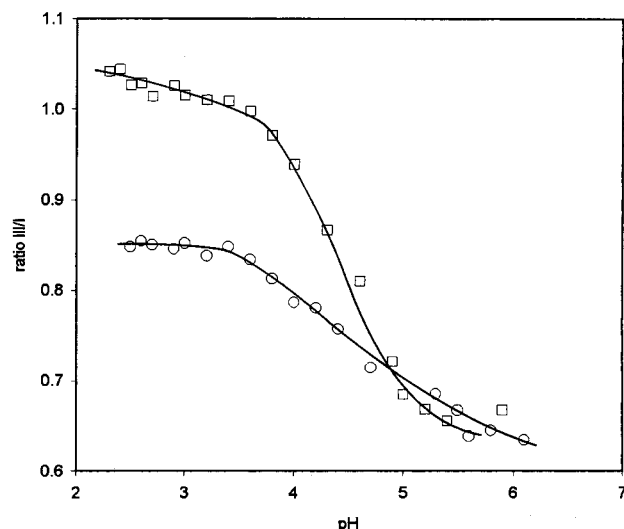


**Figure 1.** Fluorescence intensity ratio III/I of pyrene (2  $\mu$ M) as a function of pH in PMA solution (1 g/L) containing [NaCl] = 100 mM: (□) PMA540K, (○) PMA8K.

15 000 molecular weight (PMALMW) were purchased from Polysciences. Poly(methacrylic acid) sodium salts of 540 000 (PMA540K) and 8000 (PMA8K) with narrow molecular weight distribution were obtained from American Polymer Standards Corp. The polymer solutions were prepared with deionized water containing NaCl (100 mM), and the pH was adjusted with standard 0.1 N HCl or 0.1 N NaOH. The pH was measured with an Accumet combination pH electrode at 20 °C by using an Orion pH meter model SA 720.

**Instrumentation.** Steady-state fluorescence spectra were recorded on an SLM/Aminco SPF-500C spectrofluorimeter by exciting at 337 nm. The ratio III/I corresponds to the ratio of intensities of peak three ( $\lambda = 384$  nm) to peak one ( $\lambda = 373$  nm). The fluorescence decay of the singlet excited pyrene was monitored at 400 nm; following excitation with pulses from an LN100 PRA nitrogen laser, a 7912 AD Tektronik digitizer captured the emission signals observed with a Hamamatsu 928 photomultiplier. A description of the time-resolved fluorescence system has been given previously.<sup>24</sup> Kinetic fluorescence measurements were carried out on a customized adaptation of the Tri-tech Dynamic Instruments model IIA which is used in conjunction with the SLM/Aminco SPF-500C spectrofluorimeter. The spectrofluorimeter operating in the "kinetics" mode provides the capability to store up to 500 data points at 1000 points/s. The signal can also be smoothed by using a "filter" that averaged four or more points. A detailed description of the stopped-flow equipment has been given elsewhere.<sup>25</sup> All of the stopped-flow experiments were carried out at 20 °C. A pH jump was produced by mixing in this apparatus a polymer solution ([chains] = 3.7  $\mu$ M) containing NaCl (100 mM) and pyrene (1.2  $\mu$ M) with a solution of HCl (or NaOH)/NaCl (100 mM). The change in fluorescence intensity of pyrene was recorded at 390 nm after passing through a cut filter that eliminates all wavelengths below 350 nm. In all experiments 500 points, each one averaged four times, were collected at a rate of 2 points/s. Data were transferred to a PC microcomputer for storage and analysis.

## Results and Discussion

**Measurements of Steady-State Fluorescence of Pyrene.** The changes of intensity and ratio III/I in the fluorescence spectra of pyrene have been previously used to study the conformational equilibrium of PMA.<sup>10,11</sup> The plot of these spectral parameters as a function of pH is similar to those obtained by measuring equilibrium properties of the polymer system. In Figure 1 are given the results obtained for two samples of PMA of very different molecular weight: 8000 and 540 000 in

the presence of 100 mM NaCl. These plots have the same pattern found by us and other authors; i.e., the ratio III/I increases as the polymer goes from a stretched form (high pH) to a coiled state (low pH). At a pH higher than 5.0 the media sensed by pyrene is less polar in the presence of an added salt and is independent of the molecular weight of PMA. The ratio III/I at pH 6.0 is 0.55 and 0.64 in the absence and presence of salt, respectively. A value of 0.56 has been given for this ratio in an aqueous solution of pyrene.<sup>26</sup> This salt effect is produced by a reduction of the electrostatic repulsion of the ionized COOH groups. Thus, under these conditions, pyrene is not expelled to the aqueous phase but always remains in the vicinity of the polyelectrolyte. In a previous paper we have pointed out the fact that, at low pH, the limiting value of the ratio III/I was dependent on the polyelectrolyte molecular weight.<sup>11</sup> The same behavior is observed by using polymers with a very narrow distribution of molecular weights (see Figure 1). This result was ascribed to a more hydrophobic conformation, sensed by pyrene, when the polymer length chain reached a certain value. The maximum value of the ratio III/I (1.179) is reached at a molecular weight of 15 000. However, it was found that there is a polymer concentration effect on this value; i.e., the ratio III/I decreases as the polymer concentration decreases. This result suggests that there is a distribution of pyrene between a very hydrophobic region and a more polar domain. Thus, the observed ratio III/I comes from a combination of two different steady-state fluorescence spectra. The equilibrium constants for the distribution of pyrene between these two microenvironments were determined by time-resolved fluorescence measurements.

**Decay of Pyrene Fluorescence.** Pyrene (2  $\mu$ M) in aqueous solution containing 100 mM NaCl exhibits a time-dependent emission that is fitted by an expression of the form

$$I(t) = I(0) [q \exp(-t/\tau_1) + (1 - q) \exp(-t/\tau_2)] \quad (1)$$

where  $\tau_1$  and  $\tau_2$  are the lifetimes of two different exponential decays,  $q$  is the fraction of the intensity change that decays with the slower rate constant, and  $I(t)$  and  $I(0)$  are the emission intensity at time  $t$  and zero, respectively. The values of  $\tau_1$  and  $\tau_2$  are around 130 ns and 20 ns, respectively, and the fraction of excited pyrene that decays with the slower lifetime is  $0.82 \pm 0.06$  independent of the pH. It has been established that the fast part of the decay arises from the excimer formation process.<sup>27</sup> In an aqueous solution of PMA the longer lifetime of pyrene changes with pH, following the same pattern obtained with the change of fluorescence intensity or ratio III/I (see Figure 2). The shape of the curves shown in Figures 1 and 2 has been explained as a result of the conformational transition between a contracted state (at low values of pH) and an extended form occurring at higher pH. It is generally accepted that during initial neutralization the chain expands slightly, up to a value between pH 5 and 6, where the process is accelerated. Above this pH, the polymer is stated to expand with increasing charge density, and as a consequence, pyrene is released to the aqueous phase. Our data show that at pH 5.5 the lifetimes of pyrene in water and in aqueous solution of PMA are the same (130 and 20 ns) and independent of the molecular weight. However, the values of  $q$  are lower for polymer solutions than those found in water (0.82).

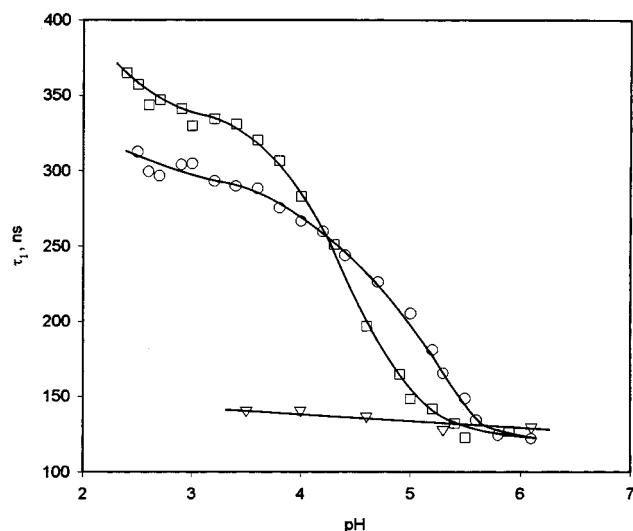


**Figure 2.** Lifetimes of pyrene ( $2 \mu\text{M}$ ) as a function of pH in PMA solution (1 g/L) containing  $[\text{NaCl}] = 100 \text{ mM}$ : ( $\square$ ) PMA540K, ( $\circ$ ) PMA8K, and ( $\nabla$ ) in aqueous solution.

This result means that a larger number of pyrene excited states can form excimers in the presence of PMA than in a simple aqueous solution. This conclusion is supported by the observation of an excimer band in the emission spectra, which intensity increases with increasing pH. These results suggest that pyrene, even at this pH, is still around the polymer (ratio III/I = 0.62) and confined to a volume where the excimer formation process is more efficient ( $q = 0.42$ ). This conclusion agrees with previous results indicating the existence of more than one structure.<sup>8,11,13</sup>

**Measurements of Pyrene Distribution Constants.** The time-resolved emission data, obtained in the region where the polymer is coiled, is also fitted by eq 1. The longer lifetime is approximately 400 ns for all polymers, except PMA8K where it is around 310 ns. On the other hand, the fast part of the decay has a lifetime ranging from 127 to 160 ns. These results indicate that pyrene is solubilized in two different locations. The partitioning of pyrene between these two environments can be described by the pseudophase model developed for micelles.<sup>28</sup> In this model it is assumed that the solute incorporation to the polymer follows a Poisson distribution, and it can be represented by the equilibrium



for which the equilibrium constant  $K_\text{C}$  is given by

$$K_\text{C} = [\text{Py}_\text{C}]/[\text{Py}_\text{P}][\text{PMA}_\text{C}] \quad (2)$$

where  $[\text{Py}_\text{P}]$  and  $[\text{Py}_\text{C}]$  denote molar concentrations of pyrene in aqueous and coiled polymer phases, respectively, and  $[\text{PMA}_\text{C}]$  is the concentration of hydrophobic coils. The coil concentration can be calculated by multiplying the chain polymer concentration by the average number of coils in one chain,  $N$ . As a consequence, we could use  $K_\text{S}$ , which is defined in terms of the chain polymer concentration, instead of  $K_\text{C}$

$$K_\text{S} = [\text{Py}_\text{C}]/[\text{Py}_\text{P}][\text{PMA}] = K_\text{C}N \quad (3)$$

A dependence of  $K_\text{S}$  on the polymer molecular weight

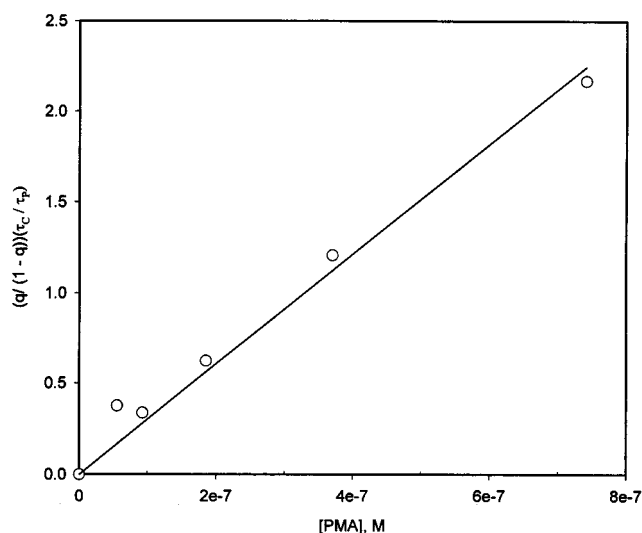


**Figure 3.** Plot of data obtained from decay of pyrene according to eq 5.  $\text{MW} = 5.4 \times 10^5$ ;  $[\text{Py}] = 2 \mu\text{M}$ .

**Table 1. Molecular Weight and Polymerization Degree of PMA Samples<sup>a</sup>**

sample	MW	PD	$\langle\tau_1\rangle$	$\langle\tau_2\rangle$	ratio III/I	$K_\text{S}, \times 10^5$
PMA8K	8 000	74	313	127	0.822	0.37
PMA1MW	15 000	139	415	161	1.179	3.84
PMAHMW	100 000	1163	417	155	1.074	32.40
PMA540K	540 000	5,000	395	130	1.040	30.30

<sup>a</sup> Average lifetimes, maximum value of ratio III/I of pyrene in PMA aqueous solution, and equilibrium constants for the distribution of pyrene between the aqueous and coil phases.

would be observed if  $K_\text{C}$  and/or  $N$  change with the polymer size.

Determination of  $K_\text{S}$  makes use of eq 1 and the following relationship between  $q$  and pyrene concentration<sup>24,29</sup>

$$K_\text{S}[\text{PMA}] = q/(1 - q)(\epsilon_{\text{Py-C}}/\epsilon_{\text{Py-P}})(\phi_{\text{Py-C}}/\phi_{\text{Py-P}}) \quad (4)$$

where the ratio of the absorption coefficients of pyrene in the different environments at the excitation wavelength is assumed to be unity, and the ratio of fluorescence quantum yield is equal to the ratio of lifetimes,  $\tau_\text{C}/\tau_\text{P}$ . This follows from the assumption that the fluorescence rate constant is the same in both media. Then, eq 4 is reduced to

$$K_\text{S}[\text{PMA}] = q/(1 - q)(\tau_\text{C}/\tau_\text{P}) \quad (5)$$

A typical plot of the right-hand side of eq 5 against  $[\text{PMA}]$  is shown in Figure 3. The values of  $K_\text{S}$  obtained from the slopes are given in Table 1. From these data it can be seen that the distribution constants change dramatically with the molecular weight ( $0.4 \times 10^5$ – $30 \times 10^5$ ) and level off for  $M_\text{w} = 1 \times 10^5$ . A similar effect has been observed in the study of solubility of polycyclic aromatic hydrocarbons in aqueous solutions of PMA.<sup>3</sup> It is worth noting that there is not a clear relationship between  $K_\text{S}$  (nor  $\log K_\text{S}$ ) and degree of polymerization. This result does not allow us to decide whether the distribution constant is mainly determined by the number of coils or the coil hydrophobicity. In comparison, values of  $K_\text{S}$  equal to  $4.5 \times 10^4$  and  $1.7 \times 10^6$  were determined for pyrene in a copolymer of maleic acid and octadecene<sup>29</sup> and in SDS micelle,<sup>28</sup> respectively.



**Kinetic Measurements of the Transition. Theoretical Model.** A linear polymer can be described as a sequence of subunits adopting only two different forms: A or B. A distribution of units between these two forms determines a state of the polymer. Thus, a transition between two states is simply a change in the number of units of each form. A cooperative transition is produced when subunits prefer neighbors of similar forms. A theory of the kinetic mechanism of a cooperative transition has been developed by Schwarz,<sup>18,19</sup> on the basis of the Zimm–Bragg model.<sup>30</sup> According to this theory the elementary steps of the transition are

- (a) nucleation: BBBB...  $\rightleftharpoons$  BBABBB  
 (b) growing: BBABBB...  $\rightleftharpoons$  BBAABB...

with equilibrium constants equal to  $\sigma s$  and  $s$ , respectively. The nucleation parameter,  $\sigma$ , is much smaller than unity, reflecting the difficulty to start a new region. The change in units fraction is given by

$$\frac{df}{dt} = \sum k f_i \quad (6)$$

where  $k$  are the unimolecular rate constants for the transformation of a unit from one form to the another. The set of linear differential equations can be solved, and a number of relaxation times may be expected. Thus, the fraction of segmental states,  $f_i$ , can be calculated as a sum of exponential functions

$$f = \bar{f} + (f^0 - \bar{f}) \sum \beta_r \exp\left(-\frac{t}{\tau_r}\right) \quad (7)$$

where  $f^0$  and  $\bar{f}$  are the fractions at times zero and infinity, respectively, and  $\beta_r$  is the weight factor of the relaxation time  $\tau_r$ . The distribution of relaxation times,  $\tau_r$ , is called the relaxation spectrum of the process, which is well described in terms of mean relaxation times defined by

$$\frac{1}{\tau^*} = \frac{\sum \frac{\beta_r}{\tau_r}}{\sum \beta_r} \quad (8)$$

$$\left(\frac{1}{\tau^{**}}\right)^2 = \frac{\sum \frac{\beta_r}{\tau_r^2}}{\sum \beta_r} \quad (9)$$

Both quantities can be determined experimentally from the data provided by chemical relaxation methods. In the transition range  $\tau^*$  and  $\tau^{**}$  satisfies the following relationships

$$\frac{1}{\tau^*} = k_f[(s-1)^2 + 4\sigma] \quad (10)$$

$$\left(\frac{1}{\tau^{**}}\right)^2 = \frac{k_f^2}{2} [(1-s)^2 + 4\sigma]^{3/2} \quad (11)$$

Accordingly, the relaxation time  $\tau^*$  shows a maximum at the midpoint of the transition, and at this point ( $s \rightarrow 1.0$ ) the relation  $(\tau^*/\tau^{**})^2 = 1/(4\sigma^{1/2})$  is obtained.

The pH-induced transition of poly(methacrylic acid) can be described with these parameters by considering

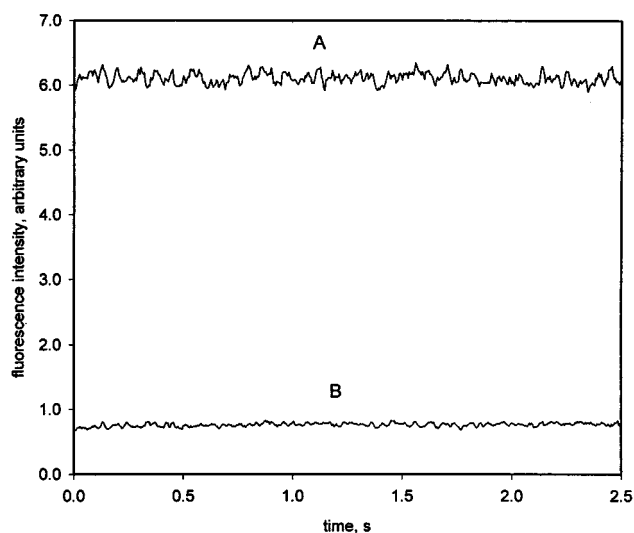
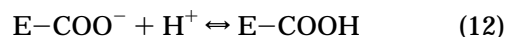


**Figure 4.** Fluorescein emission as a function of time in an aqueous solution of PMA: (A) pH = 6.2; (B) pH = 4.1. [PMA] =  $3.4 \mu\text{M}$ ; MW =  $1 \times 10^5$ ; [fluorescein] =  $6 \mu\text{M}$ .

the compact and extended states of PMA as two different distributions of hydrophobic (A form) and polar units (B form). Assuming that the fraction of segments in the A form is proportional to the pyrene emission intensity, then, a plot of intensity as a function of time allows the mean relaxation time be obtained by fitting the data to a multiexponential function. Generally, no more than two exponential are needed to fit the data.

**Kinetic Scheme for Use of Pyrene Fluorescence.** Monitoring of the PMA conformational transition, by using the fluorescence intensity change of pyrene, is based on the assumptions that both the acid–base reaction, and the entrance (or exit) of pyrene to the compact conformation adopted by the uncharged PMA, are faster than the chain movements involved in the transition. A kinetic scheme including these two processes and the transition is represented by



where E and C represent the extended and coiled states of PMA, respectively.

To verify that the reaction between  $\text{H}^+$  and  $\text{COO}^-$  groups (eq 12) occurs in a range of time shorter than 1 ms, fluorescein was used as a fluorescent probe. Fluorescein is a negatively charged indicator that shows a change of emission intensity at pH 4–4.5. This probe, because of its charge, will always stay in the aqueous phase, even in the presence of coiled PMA (pH = 3.8). Thus, any variation of pH at the bulk of solution should be detected as a change of fluorescence intensity. A comparison of kinetic traces obtained after mixing an aqueous solution of PMA, containing a sodium salt of fluorescein, with HCl and water is shown in Figure 4. It is clearly shown that the pH change is “instantaneous” and cannot be detected by the millisecond response of the stopped-flow technique.

On the other hand, the rate of entry of pyrene to the coiled form of PMA should be similar to that observed in micelles. The entrance rate constants of neutral arenes to micelles are in the range of  $(5-8) \times 10^9 \text{ M}^{-1} \text{ s}^{-1}$ .<sup>28</sup> Thus, this entry time is beyond the time resolution

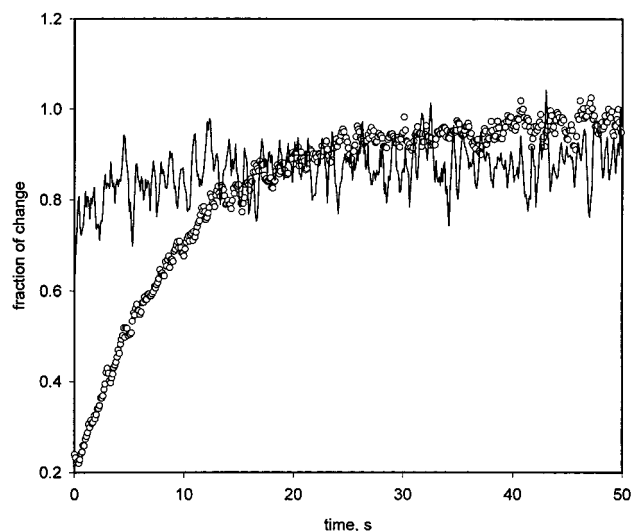


**Figure 5.** Effect of pyrene concentration on kinetic traces obtained after mixing of SDS micellar solution and aqueous solution of pyrene. [SDS] = 0.2 M. (○) [Py] = 4  $\mu$ M; (●) [Py] = 1  $\mu$ M.

of the stopped-flow equipment. However, at higher concentration of pyrene (5  $\mu$ M) a slow increase of emission intensity is observed when a PMA solution at pH 3.8 (below the transition) and an aqueous solution of pyrene are mixed. This time effect disappears at lower pyrene concentration. A similar result was observed by using a SDS micellar solution instead of PMA (see Figure 5). This pyrene concentration effect is ascribed to the dissociation of pyrene from a cluster or crystal formed at concentrations higher than 2  $\mu$ M, which occurs with a rate constant equal to  $0.07 \pm 0.01$  s $^{-1}$ .

With these results we can ensure that the changes in fluorescence intensity of pyrene, recorded by the stopped-flow equipment, reflect only the conformational transition of the macromolecule. The same conclusion was reached by Horsky and Morawetz<sup>22</sup> by measuring the energy transfer between carbazole and anthracene.

**Transition from Extended to Coiled Form.** Aqueous solutions of PMA were adjusted to an initial pH of 7–7.5 and then mixed with an amount of HCl that gave a final pH in the range where the transition takes place, i.e., 5–3.8. Figure 6 shows a typical trace of the increase in fluorescence intensity after a PMA540K solution at pH = 7.2 containing pyrene and 100 mM NaCl is mixed with HCl–NaCl to reach a pH = 3.8. The initial pH value is far above from the transition, so the intensity change observed at pH 5–3.8 is a consequence of the coiling of PMA after mixing with HCl. The emission intensity exhibits a sharp increasing in the first 5 s and then it slowly approaches a limiting value,  $I_{\infty}$ , that is reached in approximately 3 min. These intensity values are shown as horizontal lines in Figure 6. The fraction of intensity change detected kinetically is given by  $f_{SF} = (I_{\infty} - I_0)/I_{\infty}$ , where  $I_0$  is the first point recorded by the stopped-flow equipment (5 ms). The corresponding fraction in steady-state measurements is  $f_{SS} = [I(\text{pH} = 7.2) - I(\text{pH})]/I(\text{pH} = 7.2)$ . Thus, the ratio between these two quantities,  $f_{obs} = f_{SF}/f_{SS}$ , is a measure of the fraction of intensity change that can be monitored by our equipment. The values of  $f_{obs}$  obtained are given in Table 2, and they show that more than 80% of the intensity change, produced in the coiling process, can be observed by the stopped-flow method. The experimental curves of intensity against time were fit to a biexponential

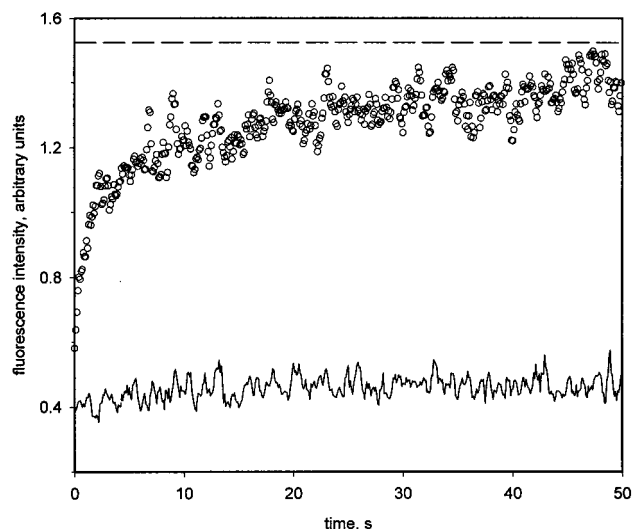


**Figure 6.** Changes of pyrene fluorescence intensity after mixing a partially neutralized PMA solution (pH = 7.2) with (○) a HCl solution and (●) water. (---) Intensity value reached at infinite time. [PMA] = 3.4  $\mu$ M; MW =  $5.4 \times 10^5$ ; [pyrene] = 2  $\mu$ M.

**Table 2. Kinetic Parameters for the Coiling Process Obtained after Mixing a PMA Solution at pH = 7.2 and 0.01 M HCl<sup>a</sup>**

sample	$f_{obs}$	$p$	$\tau^*_{max}$	$\sigma$
PMA8K	1.0	0.80	30	0.056
PMALMW	1.0	0.22	45	0.021
PMAHMW	0.85	0.18	70	0.013
PMA540K	0.80	0.48	25	0.009

<sup>a</sup> Fraction of intensity change observed by the stopped-flow technique,  $f_{obs}$ , fraction of change occurring with the faster rate constant,  $p$ , relaxation time at the mid-transition point,  $\tau^*_{max}$ , and nucleation parameter,  $\sigma$ . [PMA] = 3.7  $\mu$ M; [Py] = 1  $\mu$ M; [NaCl] = 100 mM.

kinetics according to the following equation:

$$I(t) = a + b(1 - \exp(-k_1 t)) + c(1 - \exp(-k_2 t)) \quad (15)$$

where  $k$ 's denote the rate constants and  $k_1 \gg k_2$ ;  $b$  and  $c$  are a measure of the contributions of each process to the whole change. The fraction of change,  $p = b/(b + c)$ , that occurs with a rate constant  $k_1$ , is in the range 0.2–0.8; it is independent of pH and increases with a decreasing of the polymer molecular weight. On the another hand, the rate constant of the fast part of the growth increases both with decreasing pH and by an increase in the molecular weight. For the polymer with the lowest molecular weight this component accounts for most of the change (>80%). The value of  $k_2$  is equal to  $0.025 \pm 0.005$  s $^{-1}$ , independent of pH and molecular weight. Figure 7 shows a typical growth and fit obtained for PMA540K. The contributions of each part of the growth are also depicted. These results suggest that the intensity change is produced in at least two steps. Immediately after the pH jump a fast collapse of the extended chain is produced because of the short-range interaction among the new uncharged carboxylic groups. The number of these groups is larger when the final pH is lower, and the initial process is faster. The slow approach to the final equilibrium state involves the adjustment of the coiled chains to reach a tighter conformation. It has been shown that in the presence of organic molecules the chains of PMA aggregate around the fluorescent probe forming a cluster. These

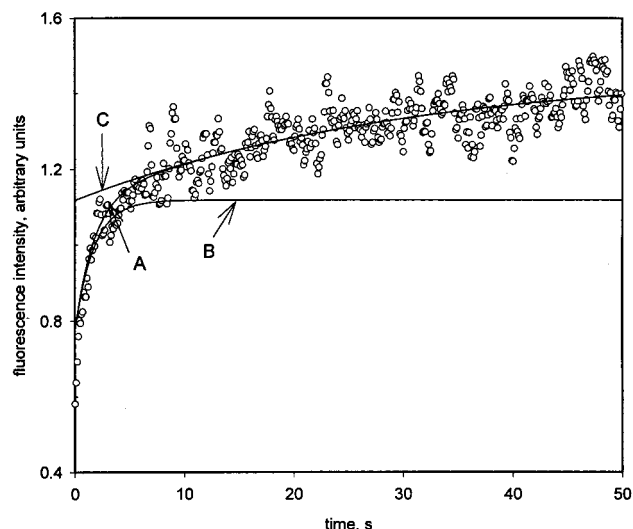


**Figure 7.** Fitting of data to a biexponential growth and comparison of the contributions from each exponential to the total change: (A) biexponential fit, (B) contribution of the fast part of the growth, (C) contribution of the slow part of the growth.

clusters are formed at low pH,<sup>13</sup> and they are stable up to pH 6.<sup>31</sup> Therefore, we can conclude that the conformational transition that takes PMA from an extended to the contracted state occurs in at least three different steps involving different structures: The first is very fast and cannot be observed by the stopped-flow technique. This step is more important for polymer with long chains. The second step is also fast, but it can be monitored during the first 10 s. These two steps involve coiled forms changing to the contracted state as a consequence of the drastic decrease of the electrostatic repulsion because of the pH jump. The final and slowest step may correspond to the clustering around the fluorescent probe.

Considering that the transition occurs through a number of different rate constants, it makes more sense to discuss the results in terms of the relaxation times, defined in eqs 10 and 11, instead of the individual rate constant values. The quantity  $\tau^*$  can be considered as a measure of the time required for the conformational transition, and  $(\tau^*/\tau^{**})^2$  is a measure of the width of the relaxation spectrum.<sup>18,19</sup> Both relaxation times can be calculated from the fitting parameters. A well-defined maximum, as predicted by eq 4, could not be observed in a plot of  $\tau^*$  against pH (see Figure 8). However, the relaxation times obtained at the midpoint of the transition are always between the highest measured values. The relaxation time,  $\tau^*$ , and the nucleation parameter,  $\sigma$ , calculated at the transition point for PMA of different molecular weights are given in Table 2. These data show that  $\tau^*$  increases with increasing chain length and then decreases for the higher molecular weight. On the other hand,  $\sigma$  increases with decreasing molecular weight. The change in  $\tau^*$  is readily understood; a longer time would be required to transform a larger number of segments from one state to the another. The short  $\tau^*$  obtained for the polymer with the longest chain could be attributed to the simultaneous occurrence of more than one coiling process. Interestingly, the values obtained for the nucleation parameter indicate that it is easier to start a hydrophobic region in a short chain polymer than in a long one. The value of  $\sigma$  obtained for PMA is smaller than the value reported for a maleic

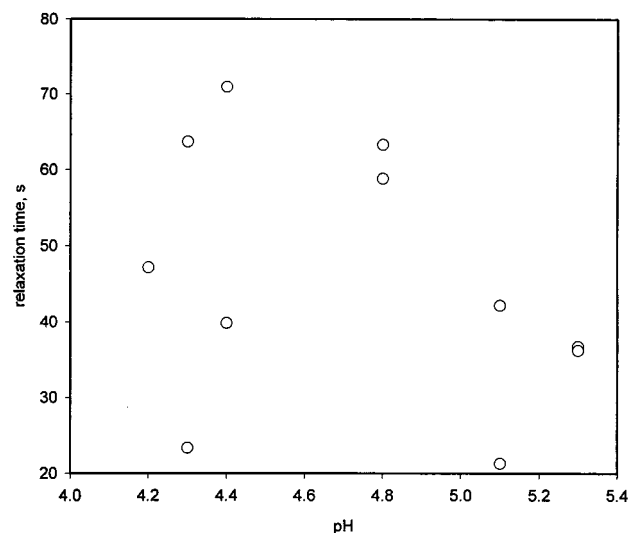


**Figure 8.** Relaxation times obtained at different values of pH, for the transition from the extended to the coiled configuration of PMA. [PMA] = 3.4  $\mu$ M; MW =  $1 \times 10^5$ ; [pyrene] = 2  $\mu$ M.

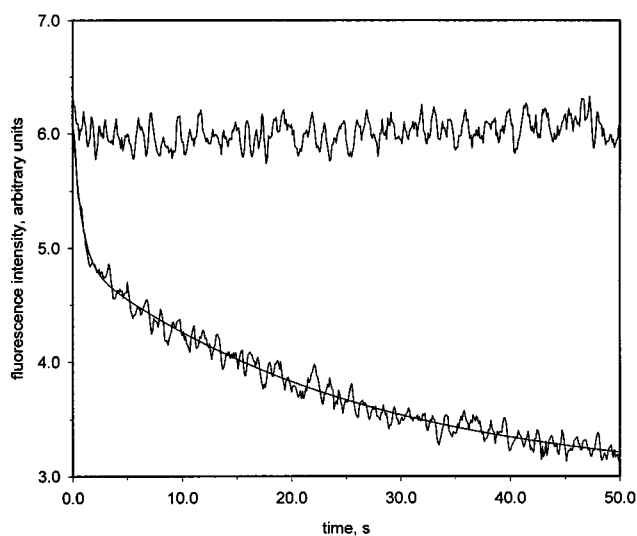


**Figure 9.** Decreasing of pyrene intensity after mixing a neutralized PMA solution with (A) water and (B) a NaOH solution. MW =  $1 \times 10^5$ ; [PMA] = 3.4  $\mu$ M, [pyrene] = 2  $\mu$ M.

acid-styrene copolymer<sup>15</sup> but still much more larger than values for the helix-coil transition if polypeptides.<sup>19</sup>

**Transition from Coiled to Extended Form.** The expansion of PMA from the contracted form (pH = 3.8) to an extended form was monitored by measuring the decrease of the emission intensity of pyrene. A kinetic trace and the fit to a double-exponential function are shown in Figure 9. The fraction of intensity change that can be followed in the stopped-flow apparatus,  $f_{obs}$ , and the relaxation times obtained for PMA of different molecular weights are given in Table 3. For the expansion process the values of  $f_{obs}$  are lower than those measured for the coiling process, indicating that in the former there is a new and very important component in eq 6 with a relaxation time shorter than 5 ms. This fast and undetected part accounts for 20–50% of the intensity change. In the observed part of the decay there is also an increase in contribution of the faster rate constant, as expressed by the  $p$  value. Obviously, the relaxation times are also shorter for the expansion than

**Table 3. Kinetic Parameters for the Expansion Process Obtained after Mixing a PMA Solution at pH = 3.8 and 0.01 M NaOH<sup>a</sup>**

sample	$f_{\text{obs}}$	$p$	$\tau_{\text{max}}^*$	$\sigma$
PMA8K	0.80	1.00	0.20	
PMALMW	0.74	0.49	10	0.018
PMAHMW	0.55	0.36	12	0.010
PMA540K	0.50	0.52	8	0.025

<sup>a</sup> Fraction of intensity change observed by the stopped-flow technique,  $f_{\text{obs}}$ , fraction of change occurring with the faster rate constant,  $p$ , relaxation time at the mid-transition point,  $\tau_{\text{max}}^*$ , and nucleation parameter,  $\sigma$ . [PMA] = 3.7  $\mu\text{M}$ ; [Py] = 1  $\mu\text{M}$ ; [NaCl] = 100 mM.

for the coiling. However, the nucleation parameters which measure the feasibility to create (or destroy) a hydrophobic pocket are almost the same for both processes. In the case of the higher molecular weight the  $\sigma$  values indicate that it is easier to destroy than to create a hydrophobic environment. The different kinetic behavior can be ascribed to the driving force producing the configuration change. In the coiling process the only force that operates is the hydrophobic attraction. On the other hand, during the first stages of the expansion there is a very strong electrostatic repulsion that originates in the ionization of the carboxylic groups. The approach to the final equilibrium state is driven by the hydrophobic interactions.

## Conclusions

For pyrene hosted in PMA aqueous solutions, the change of pyrene fluorescence intensity as a function of time reports exclusively on the kinetics of the conformational transition of the PMA chain from one mean configuration to the another. A sudden change of the degree of dissociation of PMA takes the system out of the equilibrium state as the chains cannot adopt immediately the configuration of lowest energy. So, a pH jump can be considered a perturbation of the system and the return to the equilibrium a relaxation process by which the polymer adopts the configurations corresponding to the new equilibrium state. The transition from one structure to the another is a cooperative process where polymer units become part of a hydrophobic region. This process is characterized by a distribution of rate constants, but most of the change observed in the coiling process is determined by just two relaxation times. For the expansion process there is an important part of the change that cannot be detected in the millisecond range, and this fraction increases with the polymer molecular weight. This latter process is

faster than the coiling process, and the relaxation time is almost independent of the polymer size. In the transition from an extended state to a coiled state, a longer time is observed with an increase in the number of polymer units.

**Acknowledgment.** This work has been supported by FONDECYT grant 1960920 and NSF. The travel to carry out the experiments at Notre Dame was funded by NSF/CONICYT grant 96027.

## References and Notes

- (1) Leyte, J. C.; Mandel, M. *J. Polym. Sci. A* **1964**, *2*, 1879.
- (2) Mandel, M.; Leyte, J. C.; Stadhouder, M. G. *J. Phys. Chem.* **1967**, *71*, 603.
- (3) Barone, G.; Crescenzi, V.; Liquori, A. M.; Quadrifoglio, F. *J. Phys. Chem.* **1967**, *71*, 2341.
- (4) Crescenzi, V.; Quadrifoglio, F.; Delben, F. *J. Polym. Sci. A-2* **1972**, *10*, 357.
- (5) Delben, F.; Crescenzi, V.; Quadrifoglio, F. *Eur. Polym. J.* **1972**, *8*, 933.
- (6) Katchalsky, A.; Spitnik, P. *J. Polym. Sci.* **1947**, *2*, 432.
- (7) Mandel, M. *Eur. Polym. J.* **1970**, *6*, 807.
- (8) Koenig, J. L.; Angoud, A. C.; Semen, J.; Lando, J. B. *J. Am. Chem. Soc.* **1969**, *91*, 7250.
- (9) Chen, T. S.; Thomas, J. K. *J. Polym. Sci., Polym. Chem. Ed.* **1979**, *17*, 1103.
- (10) Chu, D. Y.; Thomas, J. K. *J. Phys. Chem.* **1985**, *89*, 4065.
- (11) Olea, A. F.; Thomas, J. K. *Macromolecules* **1989**, *22*, 1165.
- (12) Heitz, C.; Rawiso, M.; Francois, J. *Polymer* **1999**, *40*, 1637.
- (13) Bednar, B.; Trnena, J.; Svoboda, P.; Vajda, S.; Fidler, V.; Prochazka, K. *Macromolecules* **1991**, *24*, 2054.
- (14) Sugai, S.; Ohno, N.; Nitta, K. *Macromolecules* **1974**, *7*, 961.
- (15) Ohno, N.; Okuda, T.; Sugai, S. *J. Polym. Sci., Polym. Phys. Ed.* **1978**, *16*, 513.
- (16) Tan, K. L.; Treloar, F. E. *Chem. Phys. Lett.* **1980**, *73*, 234.
- (17) Poland, D.; Scheraga, H. A. *Theory of Helix-Coil Transitions in Biopolymers*; Academic Press: New York, 1970.
- (18) Schwarz, G. *J. Mol. Biol.* **1965**, *11*, 64.
- (19) Schwarz, G. *Biopolymers* **1968**, *6*, 873.
- (20) Irie, M.; Schnabel, W. *Makromol. Chem. Rapid. Commun.* **1984**, *5*, 413.
- (21) Bednar, B.; Morawetz, H.; Shafer, J. A. *Macromolecules* **1985**, *18*, 1940.
- (22) Horsky, J.; Morawetz, H. *Makromol. Chem.* **1988**, *189*, 2475.
- (23) Lumry, R.; Legare, R.; Miller, W. G. *Biopolymers* **1966**, *2*, 489.
- (24) Hashimoto, S.; Thomas, J. K. *J. Phys. Chem.* **1985**, *89*, 2771.
- (25) Dowling, K. C.; Thomas, J. K. *Macromolecules* **1991**, *24*, 4131.
- (26) Kalyanasundaram, K.; Thomas, J. K. *J. Am. Chem. Soc.* **1977**, *99*, 2039.
- (27) Winnik, F. M. *Chem. Rev.* **1993**, *93*, 587.
- (28) Almgren, M.; Grieser, F.; Thomas, J. K. *J. Am. Chem. Soc.* **1979**, *101*, 279.
- (29) Chu, D. Y.; Thomas, J. K. *Macromolecules* **1987**, *1987*, 2133.
- (30) Zimm, B. H.; Bragg, J. K. *J. Chem. Phys.* **1959**, *31*, 526.
- (31) Yang, S. Y.; Green, M. M.; Schultz, G.; Jha, S. K.; Miller, A. H. E. *J. Am. Chem. Soc.* **1999**, *119*, 112404.

MA990470H